Phys. Status Solidi B **248**, No. 5, 1096–1101 (2011) / **DOI** 10.1002/pssb.201001202

physica status solidi b
www.pss-b.com
basic solid state physics

Calculations of quasi-particle spectra of semiconductors under pressure

N. E. Christensen*[,1], A. Svane[1], M. Cardona[2], A. N. Chantis[3], R. Laskowski[4], M. van Schilfgaarde[5], and T. Kotani[6]

[1] Department of Physics and Astronomy, Aarhus University, 8000 Aarhus C, Denmark
[2] Max-Planck-Institut für Festkörperforschung, Heisenbergstraße 1, 70569 Stuttgart, Germany
[3] Theoretical Division, Los Alamos National Laboratory, Los Alamos, New Mexico 87545, USA
[4] Institute of Materials Chemistry, Technical University of Vienna, Getreidemarkt 9/165TC, 1060 Vienna, Austria
[5] School of Materials, Arizona State University, Tempe, Arizona 85287 6006, USA
[6] Department of Applied Physics and Mathematics, Tottori University, Tottori 680 8552, Japan

Received 3 November 2010, accepted 4 November 2010
Published online 30 March 2011

Keywords density-functional theory, GW calculations, quasi-particle states

* Corresponding author: e-mail nec@phys.au.dk, Phone: (0045) 89423666; Fax: (0045) 86120740

Different approximations in calculations of electronic quasi-particle states in semiconductors are compared and evaluated with respect to their validity in predictions of optical properties. The quasi-particle self-consistent GW (QSGW) approach yields values of the band gaps which are close to experiments and represents a significant improvement over "single-shot" GW calculations using local density approximation (LDA) start wavefunctions. The QSGW approximation is compared to LDA bands for a wide-gap material ($CuAlO_2$) and materials with very small gaps, PbX (X = S, Se, and Te). For wide-gap materials QSGW overestimates the gaps by 0.3–0.8 eV, an error which is ascribed to the omission of "vertex corrections." This is confirmed by calculations of excitonic effects, by solving the Bethe-Salpeter equation. The LDA error in predicting the binding energy of the Cu-3d states is examined and the QSGW and LDA + U approximations are compared. For PbX the spin-orbit coupling is included, and it is shown that although LDA gives a reasonable magnitude of the gap at L, only QSGW predicts the correct order of the L_6^+ and L_6^- states and thus the correct sign (negative) of the gap pressure coefficient. The pressure-induced gap closure leads to linear (Dirac-type) band dispersions around the L point.

1 Introduction The local density approximation (LDA) [1] to the density-functional theory [2] has been extremely successful in connection with prediction of ground state properties of a large number of materials, structural, magnetic, vibrational properties including pressure effects (structural transformations [3, 4] and superconductivity, Refs. [5, 6] and references therein). The LDA, being "designed" for calculation of total energies, produces formal one electron energies which often relate poorly to optical experiments. A well-known problem is the so-called "LDA gap error" in band structures of semiconductors, where the LDA underestimates the band gap by 50–100%. Another problem, which in fact also affects ground-state properties, and which is related to underestimation of correlation, is the rather poor description of more localized *semi-core* states, like the 3d states in Zn [3, 4] and Zn compounds. Errors in the spectral position of such states affect the modeling of photoemission spectra and the states at the top of the valence band via hybridization, i.e., they also contribute to the "LDA gap error." LDA + U methods [7–9] are some ways to correct for this, and here copper aluminate, $CuAlO_2$, is chosen as an example where this problem is particularly pronounced. The Cu-3d states lie in this case in the oxygen p valence band regime and thus close to the valence band maximum (VBM). It has been shown [10] that it in fact is possible to compensate for the full LDA gap underestimate by selecting a proper effective U value. The corrected bands were used as input to calculations [10] of excitons in $CuAlO_2$ by solution of the Bethe-Salpeter equation (BSE) [11]. In less extreme cases such adjustments are not possible and in order to calculate quasi-particle states approaches like GW [12] must be applied. Hybertsen and Louie [13] presented some of the first realistic GW calculations. They used LDA wavefunctions as input. We

shall here use the self-consistent quasi-particle GW (QSGW) approximation [14–16] which, when the self-energy is iterated to self-consistency, is independent of the choice of the first (non-interacting) start Hamiltonian (usually chosen as standard LDA). Whereas the results of "one-shot" GW calculations depend on the quality of the first LDA calculation, the QSGW results do not inherit anything from the starting point. In general, the semiconductor gaps obtained by QSGW are much improved of the LDA results as well as most conventional GW calculations; see for example Refs. [14–18]. But it has also been found that the QSGW overestimates the band gaps somewhat, and this tendency is in particular significant for wide-gap materials, as for example AlN and $CuAlO_2$, Refs. [16, 17, 19].

Thus, by examining the quasi-particle states in $CuAlO_2$ we can analyze two aspects of the band gap problem in semiconductors, the influence from semicore states and the particular problems with GW corrections to gaps in wide gap materials. In addition, the delafossite $CuAlO_2$ is a technologically interesting material because it, without intentional doping is a p-type conducting, transparent oxide. Its "3R" form, which is examined here, crystallizes in a structure belonging to the $P6_3/mmc$ space group, more details in Ref. [19]. Then, as examples of semiconductors with very small energy gaps, we study the lead chalcogenides, PbS, PbSe, and PbTe (rocksalt structure). These are also of technological importance, having applications in infrared detectors, thermoelectric devices, and Tl doped PbTe may be a superconductor [20]. Relativistic LDA calculations, including spin-orbit coupling appear at a first sight to yield reasonable minimum band gaps (direct gaps at the L point in the Brillouin zone [BZ]). However, for all three compounds, the LDA gives the ordering $E(L_6^-) < E(L_6^+)$ of the band edge states which is incorrect. This means that the LDA calculations yield incorrect signs of the gap deformation potentials, and then they cannot reproduce the observations that the band gaps of these materials decrease with applied pressure [21, 22] and increase with temperature.

2 Beyond LDA: comparison of LDA + *U* and QSGW for $CuAlO_2$

2.1 Band structures Since LDA + *U* will generate a downshift of the Cu 3d states, it was examined to which extent the reduction in hybridization with the uppermost valence-band states can increase the gap to match the data obtained by optical experiments. This was done in Ref. [10], where the downshift was created by adding an orbital potential, V^{FLL}, which in the formally "fully localized limit" [8] has the form

$$V^{\mathrm{FLL}} = \frac{(U-J)(1-2\hat{n}_\sigma)}{2}, \qquad (1)$$

where $\hat{n}_\sigma$ gives the occupancy of the orbital σ, and an effective Hubbard $U_{\mathrm{eff}} = U - J$ is used instead of separate *U* and *J*. Since the occupation of the Cu 3d orbitals are larger than ½, the potential V^{FLL} shifts the d states downwards in energy. The operator $\hat{n}_\sigma$ projects out the occupancy of the orbital σ, and for a fully occupied state this gives 1, and for an empty state 0. Thus, a fully occupied state is downshifted by $U_{\mathrm{eff}}/2$. However, the Cu d orbitals in $CuAlO_2$ have occupation fractions somewhat <1 due to hybridization, and therefore the Cu 3d states are downshifted by an amount somewhat smaller than $U_{\mathrm{eff}}/2$. Figure 1 shows how the direct gaps in $CuAlO_2$ vary with U_{eff}. In Ref. [8] it was found that a choice of $U_{\mathrm{eff}} = 8.2$ eV produces a downshift of the Cu-3d density of states peak so that agreement with XPS experiments is obtained. From Fig. 1, it is seen that a similar choice of U_{eff} adjusts the lowest direct gap (at L) to a value close to that obtained [23] experimentally, ~3.5 eV.

The LDA + *U* bands are compared to the LDA band structure in Fig. 2. The inclusion of the *U* corrections clearly shifts the Cu-3d states to lower energies relative to the top of the valence band and the width is reduced. Both the LDA and LDA + *U* band structures have indirect minimum gaps, and the lowest direct gap is found at L.

Although it is possible to adjust the gap, in this particular case, to the experimental value by choosing a proper value of

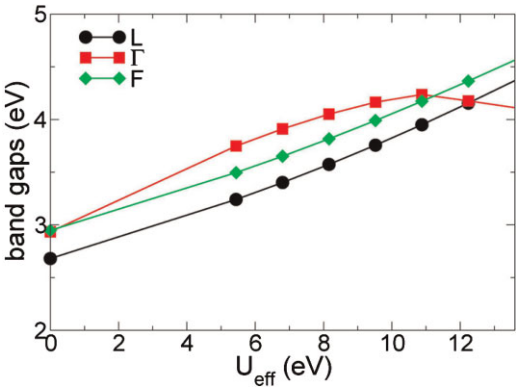

Figure 1 (online color at: www.pss-b.com) $CuAlO_2$: LDA + *U*. Direct gaps at L, Γ, and F as functions of U_{eff}.

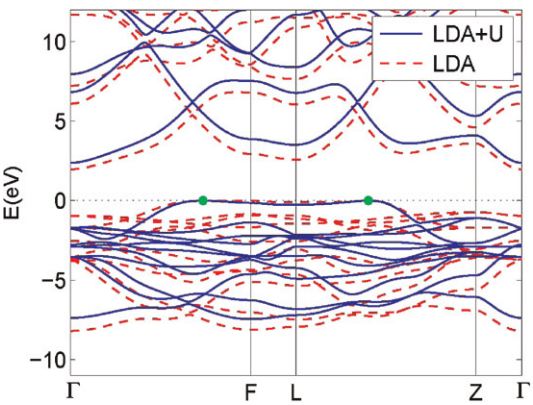

Figure 2 (online color at: www.pss-b.com) Band structures for 3R-$CuAlO_2$: LDA (red, dashed) and LDA + *U* (blue, full-line curves). The energy is zero at the valence-band maximum, indicated by the two dots (green). Spin-orbit coupling is not included in the calculations for $CuAlO_2$.

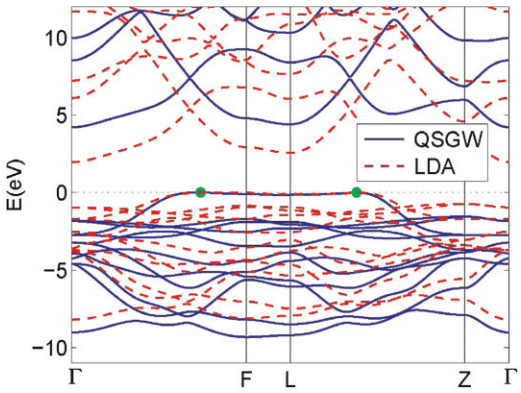

Figure 3 (online color at: www.pss-b.com) Band structures for 3R-$CuAlO_2$: LDA (red, dashed lines) and QSGW (blue, full-line curves). As in Fig. 2, the energy is in both cases set to zero at the valence-band maximum (green dots).

U_{eff} it is desirable to apply a scheme without adjustable parameters, and which is not limited to cases with high-lying "semi-core" states. The QSGW approximation is such an approach, see Fig. 3.

Like LDA + U the QSGW also shifts the Cu-3d states down in energy, but the shift is a little smaller than in the LDA + U case with gap optimizing U_{eff} value. This can be seen from Fig. 4, where the Cu-d partial density-of-states functions are shown. The shape of the LDA + U d-DOS differs from those from the LDA and QSGW calculation. This can be changed somewhat by choosing a smaller value of U_{eff}, but then the gap adjustment is lost.

The values of the gaps at four high-symmetry points, Γ, F, L, and Z are 2.90, 2.93, 2.66, and 4.28 eV, respectively, whereas the QSGW values are 5.99, 4.87, 4.55, and 7.47 eV. The smallest direct QSGW gap is 4.55 eV, i.e., 1 eV larger than the experimental value referred to earlier.

A systematic overestimate of the gaps is normal [16] for QSGW and due to the omission of higher-order terms (vertex corrections) in the GW expansion in terms of the self-energy Σ. The $e-h$ correlations are part of this, and from BSE calculations we estimated [10] the gap reduction to be

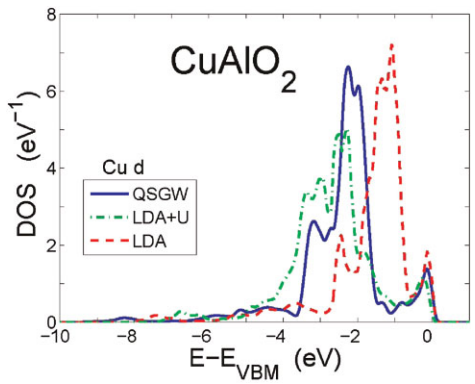

Figure 4 (online color at: www.pss-b.com) $CuAlO_2$: Cu 3d density-of-states functions calculated by the three approximations, LDA, LDA + U ($U_{\text{eff}} = 8.2$ eV), and QSGW.

$\Delta_{e-h} \sim 0.8$ eV in $CuAlO_2$. Shishkin et al. [24] calculated Δ_{e-h} for a number of semiconductors and found for GaAs 0.23 eV and for MgO, $\Delta_{e-h} = 1.04$ eV. In the latter case the gap itself is large, 7.8 eV. We have used our crude way of estimating Δ_{e-h} by examining the downshift in spectral features in the dielectric function as obtained from BSE as compared to those calculated from the bands used as input to the BSE calculation.

Some of the pressure coefficients, γ, obtained by LDA and QSGW are quite different. The LDA values for the direct gaps at the four symmetry points, Γ, F, L, and Z are 26.9, −6.1, −6.5, and 20.8 meV/GPa, respectively, whereas QSGW gives the γ values 24.5, −12.9, −13.6, and 20.4 meV/GPa. The values of γ obtained by LDA for the indirect F → Γ, L → Γ, F → L, are 19.4, 20.0, and −7.2 meV/GPa, whereas the QSGW results are 16.0, 16.3, and −14.5 meV/GPa. It is known that 3R-$CuAlO_2$ at ambient pressure is an indirect-gap semiconductor, but the smallest direct gap (at L) has a negative γ, whereas the lowest indirect gap, F → Γ, has a positive pressure coefficient. These two gaps become equal around 11 GPa (QSGW), but this does not mean that the material has a direct minimum gap at higher pressure. The indirect F → L gap has a negative γ, and it becomes the lowest gap for pressures above ∼8 GPa. The 3R structure of $CuAlO_2$ is stable for pressures up to approximately 36 GPa, and the present calculations predict that it remains an indirect gap semiconductor over the entire stability range. The lowest gap has initial states at the green dots in Figs. 2 and 3. The final state is at Γ for low pressures (<8 GPa), but it shifts to the L point at higher pressures.

2.2 Electric field gradient ^{63}Cu has the nuclear spin $I = 3/2$ and has thus a quadrupole moment. In nuclear quadrupole resonance (NQR) the electric field induced splitting of the resonance frequencies is measured, and knowing the quadrupole moment one can obtain V_{ZZ}, which is the principal component of the diagonalized electric field gradient tensor. V_{ZZ} is usually called the electric field gradient, EFG, further details in Ref. [25]. Deriving, from the NQR measurements by Abdullin et al. [26], the value of the magnitude of the EFG on Cu in $CuAlO_2$ is 10.6×10^{21} V/m^2 (the experiment does not give the sign of the EFG). Using the LDA we calculate the EFG to be -5×10^{21} V/m^2, i.e., half the measured magnitude. The EFG is, however, affected by LDA + U, and Fig. 5 shows how it varies with U_{eff}.

It is possible, in this scheme, to obtain the correct value of the EFG, but it requires that U_{eff} is set to about 13 eV, a value which is much larger than the one, 8.2 eV, which adjusts the smallest direct gap to experiment. The QSGW gives the correct value of the EFG on Cu. Figure 6 shows how the EFG varies with volume. The "LDA + 2.5 eV Cu-d downshift" is a simplified LDA + U, see Refs. [3, 4, 27].

3 PbS, PbSe, and PbTe A more detailed account on this work is given in Ref. [28].

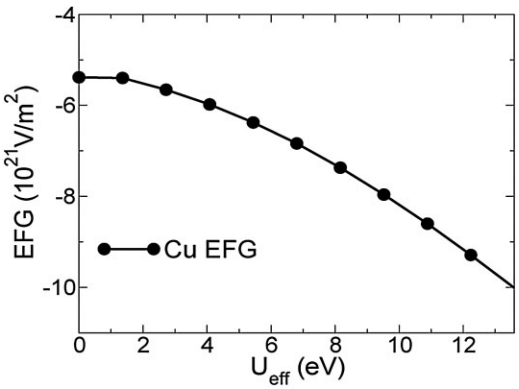

Figure 5 3R-$CuAlO_2$: the electric field gradient on Cu calculated by means of LDA + U as a function of U_{eff}.

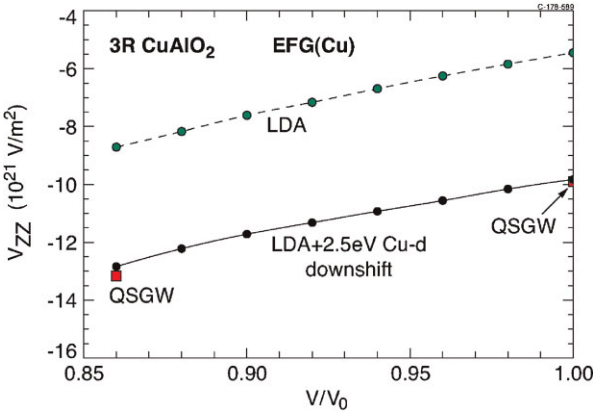

Figure 6 (online color at: www.pss-b.com) 3R-$CuAlO_2$: the electric field gradient on Cu calculated by three approaches versus volume. V_0 is the experimental equilibrium volume.

3.1 Bands, gaps at L, pressure effects The lead chalcogenides, which form in the rocksalt structure, have small band gaps, the lowest (direct), is found at the L point in the BZ. Figure 7 shows the LDA and QSGW band structures (both including spin-orbit coupling), where the low lying states, −12 eV, are of Se s character, whereas those around −8 eV are mainly Pb s. Pb p and Se p dominate the bands around the gap, and these states are strongly hybridized, and the Se states dominate below the VBM and the Pb states in the conduction bands. The minimum gap in the QSGW band structure, at L is formed by Se p states which are pushed upwards due to antibonding with Pb s, while the Pb p are pushed downward by the hybridization with Se-d states. Putting Pb at the origin, the VBM state is an even L_6^+ state while the conduction band minimum (CBM) state is an odd L_6^- state. This is the correct ordering of the gap edge states, and this is found for all three PbX compounds at ambient pressure.

The LDA and QSGW band structures in Fig. 7 look very similar, but the LDA bands have the opposite order of the edge states at L. This result of the "LDA gap error" is found

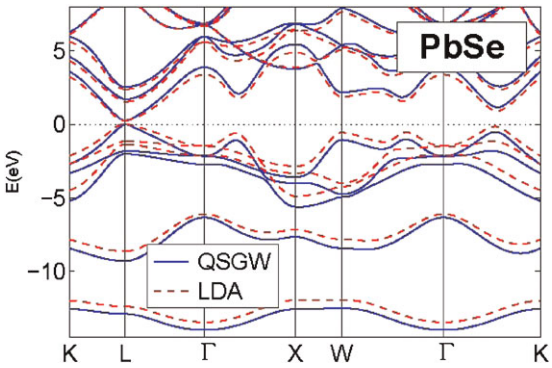

Figure 7 (online color at: www.pss-b.com) Band structures for PbSe: LDA (red, dashed lines) and QSGW (blue, full-line curves). Zero energy is set at the VBM.

for all three PbX compounds. LDA thus yields negative gap deformation potentials, whereas those from QSGW are positive. Thus, in agreement with experiments, QSGW predicts that the gaps are reduced when pressure is applied. The gap deformation potentials obtained by QSGW are 5.3, 4.9, and 3.6 eV, respectively, for PbS, PbSe, and PbTe. Using the experimental bulk moduli [29, 30], the estimated pressures at which the gaps close are $p = 4.2$, 2.4, and 3.4 GPa, respectively. The lead chalcogenides undergo pressure-induced structural transformation at $p = 2.2$, 4.5, and 6.0 GPa. Thus, the gap closure should occur at a pressure which is lower than that of the structural change in PbSe and PbTe [31]. The measured *temperature* coefficients of the gaps are $dE_g/dT = 0.45$ meV/K for PbS [32], 0.51 meV/K for PbSe [33], and 0.45 meV/K for PbTe [33]. Using the calculated deformation potentials (QSGW) together with a linear expansion coefficient (at 300 K) of approximately $2.0 \times 10^{-5}\,K^{-1}$ [34] we estimate the thermal-expansion contributions to the gap temperature coefficients to be 0.32, 0.29, and 0.22 meV/K, respectively, for PbS, PbSe, and PbTe. The experimental temperature coefficients are significantly larger, presumably reflecting significant contributions from electron–phonon interactions [33, 35]. There is experimental evidence [31] for a gapless state occurring in rocksalt PbSe and PbTe. The observed mobility behavior is in excellent agreement with the theoretical picture with the gap first shrinking to zero with pressure and then reopening upon further compression. In the entire range, 0–8 GPa studied here all three PbX compounds remain semiconductors, apart from the semimetallic state at the pressure where the gap edge states cross over. When this situation is approached the regime near L where the bands are parabolic shrinks and they become more and more linear. When the gap is zero, the bands have a perfectly linear dispersion (Dirac type). This behavior of the pressure-induced gap inversion is illustrated in Fig. 8.

The linear dispersion may have interesting consequences such as transformation into topological insulators [36] for example realized in thin films or strained bulk materials.

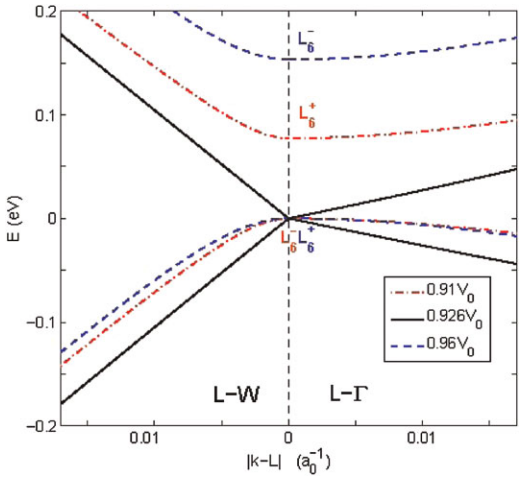

Figure 8 (online color at: www.pss-b.com) PbTe: Band dispersion (QSGW) around the L point showing the pressure-induced inversion of the gap edge states. Valence and conduction bands are shown for three volumes, $0.96V_0$, $0.926V_0$, and $0.91V_0$, where V_0 is the experimental equilibrium volume. At the largest volume (dashed blue curves) the L_6^+ state is the VBM and below L_6^-. At the smallest volume (dash-dotted red curves) the situation the opposite, and for $V = 0.926V_0$ (black, full lines) the gap is closed, and the dispersions are linear (a_0 is the Bohr radius).

3.2 Fermi surfaces of p-doped materials The band structure of PbTe, shown in Fig. 9, exhibits a local valence-band maximum at the Σ line ($\Gamma-$K) which is only slightly below the VBM. The PbSe (Fig. 7) and PbS bands exhibit a similar feature. However, in these cases, the extremum is not a maximum but a saddlepoint, and the energies are lying somewhat lower than in PbTe. Hole doping can be simulated by a rigid-band shift of the band structure, and in Fig. 10 shows a surface of con stant electron energy equal to $E_{\mathrm{VBM}} - 0.30$ eV for PbTe. From the density of states this is found to correspond to about 4% holes/f.u. This could be realized in a $Tl_xPb_{1-x}Te$ alloy alloy with

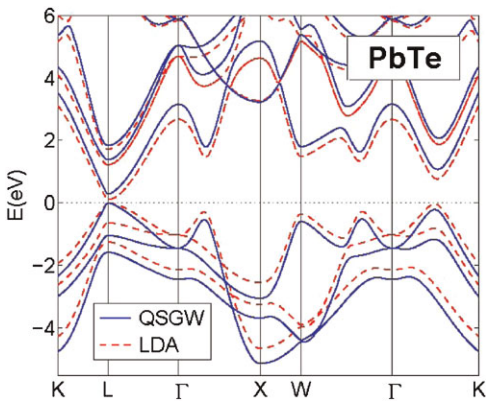

Figure 9 (online color at: www.pss-b.com) Band structures for PbTe: LDA (red, dashed lines) and QSGW (blue, full-line curves). Zero energy is set at the VBM (at the L point). $\Gamma-$K is the Σ line. Note the maximum in the valence band slightly below $E = 0$.

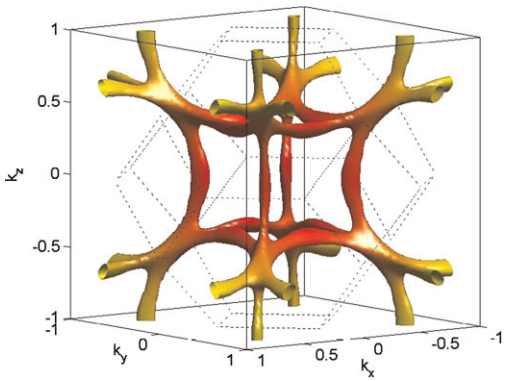

Figure 10 (online color at: www.pss-b.com) Hole surface in reciprocal space for PbTe calculated in the QSGW approximation for an energy $E = E_{\mathrm{VBM}} - 0.30$ eV. The figure is shown in a double BZ with the usual fcc BZ inside, dashed lines. The k units along the axes are $2\pi/a$, where a is the lattice constant. Colors only serve artistic purposes.

$x = 0.04$.This is somewhat above the regime where Tl doped PbTe was suggested to be superconducting [36].

One might suggest that this could be related to such a filamental Fermi surface with a large Fermi surface area and a shape which allows strong nesting. But other mechanisms of superconductivity in Tl doped PbTe have been suggested, for example that it should be due to a negative-U effect in the Tl p states [37].

Also, it has been observed [38] that the thermoelectric effect of PbTe is enhanced by addition of Tl. A large Seebeck coefficient could be related to the steep density-of-states function [28] at the Fermi level of the doped PbTe.

4 Concluding remarks Different approaches to calculations of electronic states in semiconductors have been discussed, in particular with respect to applications in theoretical studies of optical properties. This means that the formal band structures provided by the LDA are not suited, mainly due to the "gap error." It is demonstrated, by using two examples, how the QSGW approximation works as a good way to obtain reliable quasi-particle spectra, a conclusion which is supported by many other examples in the literature. The systematic, in many cases slight, overestimate of the band gaps are in wide-gap materials not negligible, but it is caused by known effects, and thus also within the possibility of calculations. A first correction is the electron-hole correlation term, not fully included in QSGW. Further, comparison between calculated electronic bands and optical spectra should take the effects of electron–phonon interactions into consideration, even the gap renormalization due to the zero-point vibrations [35]. In ZnO this renormalization is 156 meV (average of the A, B and C gap reductions) [39].

It was also demonstrated that "semi-core states" affect the band gap by hybridization to the VBM, the Cu-3d states in $CuAlO_2$ being an extreme case, though, due to their position inside the valence band. LDA + U can correct for this, the QSGW does that "automatically." Alternatively,

self-consistent self-interaction corrected (SIC) calculations [40] can be applied. Finally, it is mentioned that we did not perform calculations based on *hybrid functionals.* In that respect, the recent work by Hummer et al. [41] is particularly interesting because they apply the screened hybrid functional, HSE03, by Heyd et al. [42] to the lead chalcogenides, PbX.

References

[1] W. Kohn and L. J. Sham, Phys. Rev. **140**, A1133 (1965).
[2] P. Hohenberg and W. Kohn, Phys. Rev. **136**, B864 (1964).
[3] N. E. Christensen, in: High Pressure in Semiconductor Physics, Vol. 54 of Semiconductors and Semimetals, edited by I. T. Suski and W. Paul (Academic Press, New York, 1998), p. 49.
[4] N. E. Christensen and D. L. Novikov, Int. J. Quantum Chem. **77**, 880 (2000).
[5] N. E. Christensen and D. L. Novikov, Phys. Rev. Lett. **86**, 1861 (2001).
[6] N. E. Christensen and D. L. Novikov, Phys. Rev. B **73**, 2245 (2006).
[7] V. I. Anisimov, J. Zaanen, and O. K. Andersen, Phys. Rev. B **44**, 943 (1991).
[8] V. I. Anisimov, I. V. Solovyev, M. A. Korotin, M. T. Czyzyk, and G. A. Sawatzky, Phys. Rev. B **48**, 16929 (1993).
[9] A. I. Liechtenstein, V. I. Anisimov, and J. Zaanen, Phys. Rev. B **52**, R5467 (1995).
[10] R. Laskowski, N. E. Christensen, P. Blaha, and B. Palanivel, Phys. Rev. B **79**, 165209 (2009).
[11] L. J. Sham and T. M. Rice, Phys. Rev. **144**, 708 (1966).
[12] L. Hedin, Phys. Rev. **139**, A796 (1965).
[13] M. S. Hybertsen and S. G. Louie, Phys. Rev. B **34**, 5390 (1986).
[14] M. van Schilfgaarde, T. Kotani, and S. V. Faleev, Phys. Rev. B **74**, 245125 (2006).
[15] T. Kotani, M. van Schilfgaarde, and S. V. Faleev, Phys. Rev. B **76**, 165106 (2007).
[16] M. van Schilfgaarde, T. Kotani, and S. V. Faleev, Phys. Rev. Lett. **96**, 226402 (2006).
[17] N. E. Christensen, I. Gorczyca, R. Laskowski, A. Svane, R. C. Albers, A. N. Chantis, T. Kotani, and M. van Schilfgaarde, Phys. Status Solidi B **246**, 570 (2009).
[18] A. N. Chantis, N. E. Christensen, A. Svane, and M. Cardona, Phys. Rev. B **81**, 205205 (2010).
[19] N. E. Christensen, A. Svane, R. Laskowski, B. Palanivel, A. N. Chantis, M. van Schilfgaarde, and T. Kotani, Phys. Rev. B **81**, 045203 (2010).
[20] Y. Matsushita, P. A. Wianecki, A. T. Sommer, T. H. Geballe, and I. R. Fisher, Phys. Rev. B **74**, 134512 (2006).
[21] A. Delin, P. Ravindran, O. Eriksson, and J. M. Wills, Int. J. Quantum Chem. **69**, 349 (1998).
[22] A. H. Romero, M. Cardona, R. K. Kremer, R. Lauck, G. Siegle, J. Serrano, and X. G. Gonze, Phys. Rev B **78**, 224302 (2008).
[23] J. Pellicer-Porres, D. Kim, M. S. Lee, and T. Y. Kim, Appl. Phys. Lett. **88**, 181904 (2006).
[24] M. Shishkin, M. Marsman, and G. Kresse, Phys. Rev. Lett. **99**, 246403 (2007).
[25] A. Svane, N. E. Christensen, C. O. Rodriguez, and M. Methfessel, Phys. Rev. B **55**, 12572 (1997).
[26] R. S. Abdullin, V. P. Kal'chev, and I. N. Pen'kov, Phys. Chem. Miner. **14**, 528 (1987).
[27] N. E. Christensen and M. Methfessel, Phys. Rev. B **48**, 5797 (1993).
[28] A. Svane, N. E. Christensen, M. Cardona, A. N. Chantis, M. van Schilfgaarde, and T. Kotani, Phys. Rev. B **81**, 245120 (2010).
[29] K. Knorr, L. Ehm, M. Hytha, B. Winkler, and W. Depmeier, Eur. Phys. J. B **31**, 297 (2003).
[30] I. I. Zasavitskii, E. A. de Andrada e Silva, E. Abramof, and P. J. McCann, Phys. Rev. B **70**, 115302 (2004).
[31] V. V. Shchennikov and S. V. Ovsyannikov, Solid State Commun. **126**, 373 (2003).
[32] H. J. Lian, A. Yang, M. L. W. Thewalt, R. Lauck, and M. Cardona, Phys. Rev. **73**, 233202 (2006).
[33] G. Nimtz and B. Schlicht, Narrow-Gap Semiconductors, Springer Tracts in Modern Physics, Vol. 98 (Springer, Berlin, 1983), p. 1.
[34] O. Madelung, U. Rössler, and M. Schulz (eds.), Non-Tetrahedrally Bonded Elements and Binary Compounds I, Landolt-Börnstein New Series, Vol. III/41C (Springer, Heidelberg, 1998).
[35] M. Cardona and M. L. W. Thewalt, Rev. Mod. Phys. **77**, 1173 (2005).
[36] L. Fu and C. L. Kane, Phys. Rev. B **76**, 045302 (2007).
[37] M. Dzero and J. Schmalian, Phys. Rev. Lett. **94**, 157003 (2005).
[38] J. P. Heremans, V. Jovovic, E. S. Toberer, A. Saramat, K. Kurosaki, A. Charoenphakdee, S. Yamanaka, and G. J. Snyder, Science **321**, 554 (2008).
[39] S. Tsoi, X. Liu, A. K. Ramdas, H. Alawadhi, M. Grimsditch, M. Cardona, and R. Lauck, Phys. Rev. B **74**, 165203 (2006).
[40] A. Svane, Phys. Rev. B **53**, 4275 (1996).
[41] K. Hummer, A. Grüner, and G. Kresse, Phys. Rev. B **75**, 195211 (2007).
[42] J. Heyd, G. E. Scuseria, and M. Ernzerhof, J. Chem. Phys. **118**, 8207 (2003).